Development of p-y Curve Model for Sand Using Finite Element Analysis of Laterally Loaded Piles

Mohsen Amirmojahedi
Louisiana State University and A&M College: Louisiana State University
Murad Abu-Farsakh (cefars@lsu.edu)
Louisiana State University https://orcid.org/0000-0003-0901-6116
George Voyiadjis
Louisiana State University
Ahmad Souri
Louisiana State University

Research Article

Keywords: lateral capacity, piles, p-y curves, Finite element method, soil resistance

Posted Date: June 16th, 2022

DOI: https://doi.org/10.21203/rs.3.rs-1745746/v1

Development of p-y Curve Model for Sand Using Finite Element Analysis of Laterally Loaded Piles

Mohsen Amirmojahedi, Ph.D.[1]

Murad Abu-Farsakh, Research Professor, Corresponding Author[2]

George Z. Voyiadjis, Boyd Professor[3]

Ahmad Souri, Research Associate[4]

[1] Department of Civil & environmental Engineering, Louisiana State University, Baton Rouge, LA 70803

Email: mamirm1@lsu.edu

[2] Louisiana Transportation Research Center, Louisiana State University, Baton Rouge, LA 70808

Tel: 225-767-9147 Fax: 225-767-9108; Email: cefars@lsu.edu

[3] Department of Civil & environmental Engineering, Louisiana State University, Baton Rouge, LA 70803

Email: voyiadjis@eng.lsu.edu

[4] Louisiana Transportation Research Center, Louisiana State University, Baton Rouge, LA 70808

Email: asouri2@lsu.edu

ABSTRACT

In this study, a 3-D finite element (FE) analysis was used for estimating the lateral capacity of piles driven in sand soils. The effects of different properties of the sand on the p-y curves were studied. Using the results of FE analysis, a model for predicting p-y curves for sandy soils was developed based on the pile shape, which is a combination of tangent hyperbolic and power functions. The results of the developed model were used to demonstrate its applicability in obtaining the p-y curves for the piles driven in sand soils having increase in modulus of elasticity with depth, in sand layers with different modulus of elasticity and unit weight, and at different overburden pressures. The results of the developed model were compared to the results of full-scale pile load test that was conducted at Mustang Island, which demonstrates the ability of the model for predicting the p-y curves and lateral behavior of piles in sandy soils with good accuracy. The results of this study showed that there is little reliability on the results obtained from Reese model, which is the most common method for obtaining lateral behavior of the piles. To consider uncertainties in soil properties due to pile installation, ranges of 0.5 to 1.0 and 1.0 to 2.0 for the value of K in the developed model were proposed for non-displacement and displacement piles, respectively.

Keywords: lateral capacity, piles, p-y curves, Finite element method, soil resistance

INTRODUCTION

Piles subjected to lateral loading, sue to wind, wave, etc. will experience the horizontal shift in the whole or part of the pile and hence mobilize the resistance of the surrounding soil. The lateral load transfers from the pile to the soil through the lateral resistance of the soil, which balances the external horizontal forces and bending moments in the pile. Based on the Winkler's model (Winkler 1867), the pile can be regarded as a flexible beam on the ground rotated by 90 degrees, in which the soil resisting the lateral loads is replaced by independent springs along the pile. The stiffness of the springs, known as the modulus of subgrade reaction, is defined as follows:

$$E_{py} = \frac{p'}{y} \tag{1}$$

where p' is the force per unit length of the pile and y is the pile's deflection.

Using the Euler-Bernoulli beam theory on elastic foundations, the partial differential equation for the pile deflection under lateral loading can be obtained as:

$$E_p I_p \frac{d^4y}{dx^4} + P_x \frac{d^2y}{dx^2} + E_{py} y = 0 \tag{2}$$

where E_p and I_p are the pile's elastic modulus and second moment of area, respectively. The value of P_x is referred to the axial force, and x is the depth.

For the case of constant value of E_{py}, eq. (2) can be solved using Davisson and Gill (1963) method. For the case of sand soils, the modulus of subgrade reaction can be assumed to increase linearly with depth, as proposed by Terzaghi (1955). Matlock and Reese (1960) presented the

solutions for this case. The elastic solutions are able to predict the pile's deformation, slope, bending moment, and shear. However, the ultimate load cannot be obtained. Another technique for analyzing the lateral behavior of piles is using the ultimate load approach as proposed by several researchers such as Broms (1966) and Hansen (1961). The ultimate load approach predicts the ultimate lateral resistance of the piles; however, the response of the pile cannot be obtained.

In the p-y curve approach introduced by McClelland and Focht (1958), the value of E_{py} is not considered as a constant value, but it decreases gradually as the pile deflection progresses. The varying value of E_{py} with deflection, y, can be embedded into eq. (2); and the finite difference or finite element methods can be used to solve the pile response.

Different shape functions for p-y curves in sand have been proposed by several researchers, including hyperbolic curve (DnV 1980; Georgiadis et al. 1992; Kondner 1963; Tak Kim et al. 2004), piecewise function form (Reese et al. 1974), double broken line model (Scott 1980), power function (Wesselink et al. 1988), and hyperbolic tangent curve (API 1989; Bogard and Matlock 1980). Some of the shape functions for p-y curves proposed by different methods for sandy soils are described in **Table 1**.These p-y curves were developed based on analytical analysis and the results of full-scale load tests. Analytical methods used for obtaining p-y curves imply many simplifications such as calculations of active and passive forces from Rankin's theory from the geometry of the wedge for the failure near the ground surface and Rankin active failure condition based on two-dimensional behavior for plane-strain failure at a considerable depth below the ground surface (Reese et al. 1984; Zhang et al. 2005). The full-scale pile load tests used to back-calculate the p-y curves were conducted on a limited number of piles with specific pile diameters and soil types. For example, the most commonly used p-y curve formulations are proposed by Reese et al. (1974) and API (1989). Those p-y curves are based on the results of full-scale load tests conducted on Mustang Island, which includes tests on only two piles with the same diameter

(0.61 m). Using a database of 14 full-scale load tests performed at 10 different sites, Murchison and O'Neill (1984) showed that the predictions of pile-head deflection by Reese and API p-y curves are about 2-3 times higher than the measured data.

Table 1. Summary of some p-y curve models for sand

Finite element has been used by many researchers to investigate the lateral behavior of piles. For example, Ashour and Norris (2000), Uncuoğlu and Laman (2011), Conte et al. (2013) studied the effects of different soil and pile parameters on the p-y curves; however, they did not propose any equation.

In this study, the results of 3D finite element analysis were used to study the effects of different soil parameters on p-y curves in sands. Different models for different shapes of piles were proposed for p-y curve formulation. The applicability of the models for the case of layered sand soils, and overburden pressures were also investigated. The results of full-scale pile load tests at Mustang Island were analyzed by the developed model, which shows that the proposed model is able to back-calculate the p-y curves from field tests.

FINITE ELEMENT NUMERICAL MODEL

The pile (circle shape with diameter D) and the surrounding soil are modeled in a three-dimensional finite element program, ABAQUS. The finite element grid and boundary conditions are shown in **Figure 1**. Mesh sensitivity was first conducted to find the optimum mesh-size and degree of refinement where the numerical results are not mesh-size dependent. Using the mesh size analysis, the size of the elements close to the pile was created smaller than the elements far from the pile. As shown by Duncan et al. (1994) and Christensen (2006), the lateral behavior of

piles is significantly dependent on the properties of soil within a zone varying from ground surface down to 8D to 10D below surface. Therefore, p-y curves for soil to depth, x=15D were obtained and studied in this research. Based on sensitivity analysis, a depth of 18D and radius of 40D were selected for the FE model to minimize the effects of boundary conditions on the pile response. The lateral boundaries were fixed by roller support to prevent the soil movement in the horizontal direction. The bottom of the soil domain was fixed by roller support to prevent the soil from movement in vertical direction. Only half of the pile and soil was modeled due to symmetry which significantly reduces the solution time.

Figure 1. (a) Three-dimensional schematic of the pile-soil model for finite element analysis (b) section xy of the model (c) section yz of the model

Element type of C3D8R (eight-node linear brick element, reduced integration) was selected for soil elements, which provides linear interpolation of displacements in each direction. Soil material was modeled by elastic-perfectly plastic model of Mohr-Coulomb (M-C) with no cohesion. M-C criterion is simple in formulation and there are a lot of experimental data available for its input parameters, especially for sand soils. Pile material was modeled using elastic properties considering the elastic modulus of E_p=2,000 GPa and Poisson's ratio, $\nu = 0.15$. A high value of E_p was selected, so that no deflection in pile occurs during moving laterally the top and bottom of the pile simultaneously, as shown in **Figure 2**. The Coulomb interface model available in ABAQUS was adapted in this study. The model is able to transfer the normal and shear forces along the pile and soil surfaces. "Hard contact" rule governs in the interface contact that allows the transfer of shear stresses between surfaces, no transfer of tensile normal stress, and relative displacement of pile-soil interface when the shear stress reaches to the bond strength based on Coulomb frictional contact law. Coulomb friction model assumes no relative motion if the

134 frictional stress is less than critical stress, $\tau_{cr} = \mu\sigma_n$, where σ_n is the normal contact pressure and
135 μ is the friction coefficient. The selected values of model parameters used in this study are
136 presented in **Table 2**. These values are selected based on typical properties of soils presented in
137 Appendix C of Subramanian (2008).
138
139 **Table 2. Model parameters used in the finite element analysis**
140
141 The simulation was performed in two steps. In the first step, the geostatic stress in the soil
142 was established by applying gravity load (g=9.81 m/s^2) and the global stress equilibrium was
143 achieved. In the second step, the whole pile was pushed laterally in order to get a complete form
144 of p-y curve. **Figure 2** presents the steps of obtaining p-y curves from the results of pile-soil FE
145 model that was adopted to perform the parametric study. For this purpose, sampling points at equal
146 distances were chosen to measure the pile shear at different steps during pushing the pile. At each
147 step, a curve was fitted to the pile shear values using a suitable curve fitting technique. For this
148 purpose, cubic spline fit was adopted in this study, which has been shown to produce more accurate
149 fit with less severe oscillations between data points than high-order polynomial fits (Haiderali and
150 Madabhushi 2016). The soil resistance profile was then obtained by taking the derivative of shear
151 curve. The p-y curve at each depth was determined by collecting the values of soil resistance over
152 the steps of applying pile lateral displacement (**Figure 2**).
153
154 **Figure 2. Procedure of obtaining soil resistance from results of finite element at a specific**
155 **displacement for calculating p-y curves**
156

P-Y CURVE MODEL IN SANDS

In this study, a simple equation form for p-y curves in sands was assumed by introducing a power function inside the hyperbolic tangent function, as shown below:

$$p = p_u \, tanh\left[\left(\frac{\alpha y}{y_{ref}}\right)^n\right] \tag{3}$$

where p is the soil reaction, y is the displacement, p_u is the ultimate soil resistance, and y_{ref} is the reference deflection. In the above equation, when $y = y_{ref}$, the value of p becomes equal to $p_u \, tanh(\alpha^n)$. When the value of $\alpha = 2$ and $n = 1$, the soil resistance reaches to $0.96p_u$ at $y = y_{ref}$. Accordingly, the y_{ref} value can be defined as the displacement when the soil reaction, p reaches to the ultimate value, p_u. By fitting eq. (3) to p-y curves obtained from FE analysis, while α value is set to 2.0, the values of p_u and y_{ref} can be obtained. The estimation of reference deflection, y_{ref}, for the p-y curve in eq. (3) is easier compared to estimating the value of initial slope of the p-y curve, k_{ini}. The value of k_{ini} can be determined by computing the derivative of equation (3) at $y = 0$.

PARAMETRIC STUDY ON P-Y CURVES IN SANDS

In this study, the effects of different soil and pile parameters on the lateral behavior of piles were investigated. This includes the elastic modulus of soil (E_s), Poisson's ratio of soil (ν), angle of internal friction of soil (φ'), effective unit weight of the soil (γ'), soil-pile interface friction coefficient (μ), coefficient of lateral earth pressure (K), and pile width (D). The range values of these factors used in the parametric study are presented in **Table 2**. In studying each parameter, the value of that parameter was changed to different values in **Table 2**, while the other parameters kept as the bolded values in the table (as reference case).

Effect of soil elastic modulus

Typical range of soil elastic modulus values for silt, silty sand, loose, and dense sand are 2-20, 7-21, 10-24, and 48-81 MPa, respectively. In this study, the parametric study for the values of E_s equal to 9.6, 23.9, 47.9, and 95.8 MPa was conducted, which represents silty, loose, medium, and dense sands; respectively. Figure 3 shows p-y curves obtained from the 3-D FE analysis.

As shown in Figure 3, the ultimate soil resistance, p_u increases with depth and does not change with varying values of modulus of elasticity, E_s. However, the reference deflection, y_{ref} increases with depth, while decreases with increasing the modulus of elasticity, E_s. For example, for depth x=4D, the obtained values of p_u for are 504, 498, 492, and 492 kN/m for E_s values of 9.6, 23.9, 47.9, and 95.8 MPa, respectively. On the other hand, for depth x=4D, y_{ref} values decreases from 442 mm for E_s=9.6 MPa to 49 mm for E_s=95.8 MPa.

Figure 3. The p-y Curves for piles in sands with elastic modulus (E_s) (a) 9.6 (b) 23.9 (c) 47.9 (d) 95.8 MPa

Effect of soil Poisson's ratio

Typical values for Poison's ratio for silt, fine sand, coarse sand, and dense sand are 0.3-0.35, 0.25, 0.15, and 0.2-0.4, respectively. The 3-D FE model was used to develop p-y curves for these different ν values of 0.2, 0.3, and 0.4. Obtained p-y curves shown in Figure 4a shows that Poison's ratio has negligible effect on the values of both p_u and y_{ref}. For this case in different values of ν values, the obtained values of p_u and y_{ref} in depth x=4D were obtained as 498 kN/m and 189 mm, respectively.

Effect of soil internal friction angle

The range of values of angle of friction, φ' for very loose, loose, medium, dense and very dense

sands are < 29°, 29°-30°, 30°-36°, 36°-41°, and > 41°, respectively. 3-D FE analysis was conducted to develop p-y curves for sand soils with $\varphi' = 25°$, 30°, 35°, and 40°.As shown in Figure 4b, the value of p_u increases significantly with increasing φ'. For example, by increasing the value of φ' from 25° to 30°, the value of p_u increases from 352 kN/m to 498 kN/m, which is about 40% increase in p_u. This shows the results are very sensitive to the soil internal friction. Also, at higher values of φ', the whole p-y curve is not fully activated, which implies that y_{ref} also increases.

Effect of soil effective unit weight

Typical values of unit weight of loose and dense sands are 17.5 kN/m^3 and 20.5 kN/m^3, respectively. Having the value of unit weight of water as 9.81 kN/m^3, different values of effective unit weight, γ' equal to 7.9 and 9.4 kN/m^3 for saturated soil, and 15.7 and 18.9 kN/m^3 for dry sand were used to develop p-y curves in 3-D FE analysis. Figure 4c presents that both the values of ultimate soil resistance, p_u and reference deflection, y_{ref} increases with increasing the effective unit weight. The value of p_u increases from 498 kN/m to 627 kN/m with increasing γ' from 7.9 kN/m^3 to 9.4 kN/m^3. Meanwhile, the value of y_{ref} increases from 189 mm to 256 mm with increasing γ' from 7.9 kN/m^3 to 9.4 kN/m^3.

Effect of soil-pile interface friction coefficient

Different values of interface friction angle for the pile-soil, δ, have been proposed by different researchers. For the case of steel and formed concrete piles, δ varies from 11-14° for silts to 17° for sands. However. for the case of piles made of mass concrete, the range of δ values of 17-19°, 19-24°, 24-29°, and 29-31° are suggested for silt, fine sand, medium sand, and coarse sand, respectively (NAVFAC 1982). Another recommended values for interface friction angle is related to the friction angle of the soil, φ' and pile material. The values of δ for different pile materials including rough concrete, smooth concrete (precast piles), rough steel, smooth steel, and wood

(timber piles) are 1.0φ', (0.8-1.0)φ', (0.7-0.9)φ', (0.5-0.7)φ', and (0.8-0.9)φ', respectively. In this study, three interface friction angles of 17°, 22°, and 27° with corrsponding interface friction coefficients, $\mu = \tan\delta$ of 0.3, 0.4, and 0.5 were selected in the FE parameter study. The results of p-y curves are presented in Figure 4d, which shows that the interface friction angle does not have significant effect on the p-y curves of piles driven in sand soils. This can be attributed to the fact that the soil resistance to the lateral movement of the pile has two components: the frontal normal reaction and the side friction resistance (Smith 1987). The effect of later component developed from shear drag is much less than frontal normal reaction as some researchers such as Terzaghi idealized the problem by assuming uniform pressure in front of the pile and neglecting the shear drag (Terzaghi 1955). The obtained results shown in Figure 4d is in agreement with those assumptions.

Effect of lateral earth pressure coefficient

Most of the analytical methods that are used to determine the p-y curves for piles in sands assume that the coefficient of lateral earth pressure, K of the soil surrounding the pile is equal to the at rest coefficient, K_0. For example, this value in Reese method has been assumed to be 0.4. However, it should be noticed that this value can be increased significantly for the case of overconsolidated soil and due to the effect of installation for displacement piles. In this study, four K values of 0.5, 0.75, 1.0, and 2.0 were selected FE analysis and the resulting p-y curves are shown in Figure 4e. The figure clearly demonstrate the significant effect of K values on the ultimate resistance, p_u and the reference deflection, y_{ref}, such that p_u and y_{ref} increase with the increase of K. For example for case of x=4D shown in Figure 4e, by increasing K from 0.5 to 0.75, the value of p_u increased from 2165 kN/m to 535 kN/m, and y_u increased from 225 mm to 288 mm.

Effect of pile diameter

In this study, three different pile diameters of 0.61, 0.91, and 1.22 m were selected to investigate

the effect of pile diameter on the p-y curves of piles driven in sand soils and the results are presented in Figure 4f. It can be seen that increasing the pile diameter leads into significant increase in both the values of p_u and y_{ref}. Comparing the values of p_u at the same depth x=3.66 m shows that by increasing pile diameter from 0.30 m to 1.22 m, the value of p_u increases from 243 kN/m to 585 kN/m, and y_{ref} increases from 100 mm to 190 mm.

Figure 4. Effects of (a) Poisson's ratio (b) friction angle (c) effective unit weight (d) interface friction (e) coefficient of lateral earth pressure (f) pile's diameter on the p-y curve at depth, x=3.66 m

Effect of pile shape

The effect of pile shape on p-y curves was investigated using three different shapes, i.e. circular, square, and rhombus. 3-D FE numerical analysis was performed to determine the p-y curves for these pile shapes at different depths. Figure 5 presents the results of p-y curves for different shapes at different depths of 0.91, 1.83, 3.66, and 9.14 m. The results show that generally at low lateral displacements, the lateral soil resistance activated for the circular piles are higher than rhombus and square piles. However, continuing moving the pile laterally, for some depths (i.e. 0.91 and 1.83 m), the mobilized lateral soil resistance of the square pile becomes higher than the rhombus and circular piles. This results demonstrate that the shape of p-y curves is highly dependent on the pile shape. Therefore, different p-y curve models are needed to be developed for different pile shapes.

Figure 5. The p-y curves for circular, square, and rhombus pile at depth (a) 0.91 (b) 1.83 (c) 3.66 (d) 9.14 m

DEVELOPING MODELS FOR P-Y CURVES IN SAND

For developing nonlinear regression models for p-y curves in sand, the results of parametric study were used for estimating a relationship based on equation (3). The nonlinear regression analysis is a form of statistical model by which a dataset can be easily visualized and explained in regression equations (Bethea 2018; Chatterjee and Hadi 2015; Motulsky and Ransnas 1987; Ratkowsky and Giles 1990; Rojas 2013; Shojaeizadeh et al. 2018; Soleimani et al. 2019). The terms L_0=1 m (3.28 feet), γ_w=9.81 kN/m^3 (62.43 pcf), and σ_{atm} =101 kPa (2116 psf) was added to the equations in attempt to make the equations dimension-less. Table 3 presents the results of regression analysis for the pile shapes (circular, square, and rhombus) in terms of models for evaluating the ultimate soil resistance, p_u, and reference displacement, y_{ref}. The α parameter in equation (3) for all pile shapes was set to 2.0, while the n parameter was determined to be 0.8, 0.66, and 0.8 for the circular, square, and rhombus, respectively.

Table 3. Developed model for p-y curves in sands for different pile shapes

It should be noted here that the rhombus piles can be thought of as square piles when the applied displacements in two lateral directions are equal to each other (i.e. diagonal resultant direction), as shown in Figure 6; while the p-y curves in Table 3 for square piles are for the case when lateral displacement is applied in only one direction. In case of unequal multidirectional lateral loading on square piles, appropriate interpolation between p-y curves obtained from square and rhombus piles can be used.

Figure 6. Square piles under multidirectional lateral loading

APPLICATION OF THE DEVELOPED P-Y CURVES IN VARYING SUBSURFACE SOIL CONDITIONS

It is very common to consider an increase in E_s with depth in sands, especially in top sand layers. In addition, different sand layers with different E_s values along the pile length occur in the field. Other than changes in E_s, another common irregularity in the field is the variation in the effective unit weight, γ'. Depending on the depth of groundwater level, γ' above and below the groundwater table will be different. Another phenomenon that can also change the p-y curve functions is applying overburden on the ground surface. The effect of these conditions will be discussed in this section to demonstrate how the developed p-y models in previous section can be implemented in different subsurface soil conditions in the field.

In this analysis, the value of E_s was assumed to increase from zero at the ground surface to the value of 23.9 MPa at depth x=16.5 m. The linear increase of E_s with depth known as Gibson-type profile (Gibson 1967; Mayne and Poulos 1999), can be described by the eq. (4) as:

$$E_s = A\sigma'_{vo} \tag{4}$$

where the range of values of A for loose, medium, and dense sands are 100-300, 300-1,000, and 1,000-2,000, respectively. As can be seen from p-y curve functions in Table 3, the value of p_u does not change with E_s. On the other hand, the value of y_{ref} decreases with increase in the E_s value. FE analysis were conducted for the case of E_s increase with depth and the results are compared with p-y model presented in Table 3. Figure 7 presents the comparison between the FE analysis and the developed p-y model for this case (linear increase in E_s with A=308), which demonstrates that the developed p-y model is able to capture FE results.

Figure 7. Comparison between p-y curves of Finite Element and model for the case of E_s increases linearly to 23.9 MPa (1,000,000 psf) at Depth 16.5 m (54 ft)

For studying the effect of soil layers with different modulus of elasticity, E_s, the soil model

was divided into three regions from depth 0 to 5.5, 5.5 to 10, and 10 to 16.5 m. Two cases were investigated. The first case consists of top and bottom strong layers with E_s=47.9 MPa and middle weak layer with E_s=9.6 MPa. The second case consists of top and bottom weak layers with E_s=9.6 MPa and middle strong layer with E_s=23.9 MPa. The results of p-y curves obtained from finite element analysis and the developed p-y model in Table 3 are used to calculate the increase in soil resistance with depth as shown in Figure 8.

Figure 8. The value of soil resistance, p for piles in layered sands with different modulus of elasticity

For the case of weak middle layer in Figure 8a, the values of soil resistance profile for lateral displacement, y=0.1 m was obtained. It can be seen that the soil layers with higher E_s values reached to the ultimate value, p_u, but the middle layer with lower E_s value did not reach to the ultimate resistance. Figure 8b depicts the profile of soil resistance along the pile at lateral displacement of y=0.3 m for the case of middle layer with higher E_s value than the top and bottom layers. It can be seen that both the top and middle layers reached almost to the ultimate resistance, p_u, while the soil resistance for the bottom layer did not reach to the ultimate value. The results of this analysis for linearly increase of E_s with depth, demonstrates that the developed p-y models are able to predict the lateral behavior of the piles in layered sands with good accuracy.

The equivalent depth method proposed by Georgiadis (1983) can be used for soil layers with different unit weights. In this method, the values of p_u and y_{ref} for the first layer were established using the same procedure in homogenous soils. For the second layer, the equivalent depth, h_{eq} at the top of this layer should be evaluated. For this purpose, the force required to induce soil failure in the top layer is calculated. Then the equivalent depth, h_{eq} is back-calculated by introducing the second layer properties in the force calculations. Eq. (5) describes the basic

equation for calculating h_{eq}.

$$\int_0^{h_{eq}} p_{u2}(x)dx = F_1 = \int_0^{H_1} p_{u1}(x)\,dx \tag{5}$$

where $p_{u1}(x)$ and $p_{u2}(x)$ are the ultimate soil resistance at depth x using the first and second layer properties, respectively; and H_1 is the thickness of the top layer.

Using the developed model for circular piles in Table 3, the value of h_{eq} can be obtained as follows:

$$h_{eq} = H_1\left(\frac{\gamma_1'}{\gamma_2'}\right)^{0.263} \tag{6}$$

With h_{eq} determined, variation of p_u and y_{ref} in the second layer can be obtained by replacing depth, x in the model equations by $h_{eq} + x - H_1$. The same procedure should be followed for the next layers with different values of unit weights.

Based on eq. (6), depending on the overlying soil properties, the equivalent depth can be higher or less than the actual depth. In this study, the Georgiadis method was applied for two different cases: the first case consists of top layer with γ'=18.9 kN/m^3, middle layer with γ'=7.9 kN/m^3, and bottom layer with γ'=9.4 kN/m^3. The second case consists of top layer with γ'=15.7 kN/m^3, middle layer with γ'=18.9 kN/m^3, and bottom layer with γ'=9.4 kN/m^3. The results for soil resistance for these two cases are shown in Figure 9a and b for displacements of 0.31 and 0.29 m, respectively. It can be seen from Figure 9 that applying the eq. (6) to the developed p-y curve model is capable of reproducing finite element results with good accuracy.

Figure 9. The value of soil resistance, p for piles in layered sands with different unit weight

The model was tested to see if it is able to reproduce the same results for the case of

overburden pressure, σ'_0. For this purpose, a modified method was used to estimate the equivalent depth. At each depth, the value of effective unit weight, γ' was changed by eq. (7), so the same vertical pressure at each depth was obtained.

$$\gamma'_{eq} = \gamma' + \frac{\sigma'_0}{x} \tag{7}$$

The procedure described for eq. (6) in previous section was then used to obtain the equivalent depth. The results of this method for σ'_0=47.88 and 95.76 kPa are shown in Figure 10a and b at pile lateral displacements of 0.3 and 0.32 m, respectively. Figure 10 suggests that the developed p-y model is able to capture p-y curves for the case of varying overburden pressure with acceptable accuracy. However, it seems that the p-y model slightly underpredicts the soil resistance at shallow depths and slightly overpredicts the soil resistance at deep depths. It can be also noticed that the difference between the model and the finite element results increases with increasing the overburden pressure.

Figure 10. The value of soil resistance, p for piles in sands with overburden pressure, σ'_0 equal to (a) 47.88 (b) 95.76 kPa

VERIFICATION OF THE DEVELOPED P-Y MODEL FOR SAND

To verify the developed p-y model, a full-scale pile load test conducted at the Mustang Island near Corpus Christi, Texas, described by Cox et al. (1974) was compared with the results of p-y models. The steel pile with embedment length of 20.7 m and diameter of 0.610 m was installed open-ended, which helps to reduce the changes in soil properties. The soil was uniformly graded fine sand with a friction angle of 39° and a relative density, D_r= 0.9. The submerged unit weight was 10.4 kN/m^3 and the water surface was kept 150 mm above the ground surface during the test. The elastic

properties of the medium dense sand based on Janbu equation (Janbu 1963) is $E_s = \overline{K}\sigma_{atm}(\sigma'_m/\sigma_{atm})^n$ with $\sigma'_m = ((\sigma'_1 + \sigma'_2 + \sigma'_3)/3)$ and $\nu = 0.3$. The values of $\overline{K}$ and n were chosen to be 1200 and 0.7, respectively; based on the estimations of Fan and Long for medium dense sand of this site (Fan and Long 2005). In this study, different values of coefficient of lateral earth pressure, K equal to 0.4 and 1.0 was assumed in the proposed p-y model's equations. The comparison between the measured and predicted p-y curves at depth x=0.3 m are shown in **Figure 11**. In addition to the results of the proposed p-y model, p-y curves obtained from Reese analytical and Reese models (described in **Table 1**) are presented in **Figure 11**, too. Reese analytical model is based on wedge failure at shallow depths and flow around failure and leads into theoretical ultimate resistance, p_c. However, Reese et al. (1974) found a poor agreement between p_c and the results of full-scale tests at Mustang Island. Therefore, they introduced an empirical factor, A, which converts the analytical solutions to fit the measured data. The factor A can be estimated using a chart or table or approximated using eq. (8) (Murchison and O'Neill 1984; Van Impe and Reese 2010; WSD 1993).

$$A = \left(3.0 - 0.8\frac{x}{D}\right) \geq 0.9 \quad (8)$$

Reese et al. (1974) did not provide any specific explanation for the reason of the difference between the analytical and measured values of ultimate soil resistance. The difference can be attributed to the simplifications used in Reese analytical solutions such as assumptions for K_0=0.4 and $K_a = tan^2\left(45 - \frac{\varphi}{2}\right)$. In addition, some other assumptions were used that neglects the effects of load type and pile surface roughness (Brødbæk et al. 2009). Another explanation is the change of soil properties after pile installation. The values of elastic modulus, friction angle, and lateral pressure of the surrounding soil usually changes due to pile driving, vibration, and soil expansion. For the case of pile load test at Mustang Island, the use of open-ended steel pile would minimize

soil disturbance caused by soil expansion and friction between the pile and the soil. However, still there is a possibility that driving the pile and associated vibration can disturb the surrounding soil and even create a gap between the pile and soil.

The use of K values of 0.4 and 1.0 in the proposed p-y model, showed acceptable range of p-y curves in **Figure 11**. It should be noticed that the measured p-y curve shown in **Figure 11** is obtained by Reese and Cox (1969) method of curve fitting for uninstrumented piles using only deflection and rotation at the pile head with some assumptions (Van Impe and Reese 2010). Therefore, some errors are possible for the measured data points.

As can be seen from **Figure 11**, the analytical solution of p_c by Reese at shallow depths is less than the measured data and the predictions of the proposed p-y model. By increasing depth, the value of p_c by Reese analytical solution gradually increases, until it reaches to the measured data at a depth x=1.83 m (x/D=3). At deeper depths, the values of Reese analytical solution becomes higher than the measured data and the proposed p-y model predictions. These changes explain the changes in parameter A factor proposed by Reese from 2.9 at surface to 0.88 at depths of x/D>5. Meanwhile, **Figure 11** clearly demonstrate that the developed p-y model can predict the measured data with acceptable accuracy using K=0.4 and K=1.0. Based on these results, it is obvious that the value of p_u ranges between the p-y model predictions of K=0.4 and 1.0.

Studying the initial slope of p-y curves at shallow depths in **Figure 11** shows that the slope of the developed model is less than the measured data values. However, with increasing depth, the initial slope of the developed p-y model increases until the p-y curve for K=1 becomes closer to the measured data at depth x=2.44 m (x/D=4). **Figure 11**g shows that at a deeper depth, the initial slope for K=1 curve becomes higher than the measured data; while the K=0.4 curve is able to predict the initial slope better. It should be noted here that the initial slope for Reese method, is not based on analysis, but rather it has been suggested for different sand types (i.e., Loose, medium,

and dense sands below or above the water table).

Figure 11. Comparison between the measured and predicted p-y curves for depths, x= (a) 0.30 m (b) 0.61 m (c) 0.91 m (d) 1.22 m (e) 1.83 m (f) 2.44 m (g) 3.05 m

Selecting appropriate values for soil properties such as the angle of friction, φ' and the coefficient of lateral earth pressure, K for use in the p-y model is not an easy task. In fact, the pile installation method has significant effect on these properties. For example driven piles in loose sand densify the soil and increase the lateral effective stresses; whereas bored piles might reduce these values (Mayerhof 1976). Budhu and Davies (1987) suggested the following equation for correcting the angle of internal friction in case of driven piles:

$$\varphi' = 15 + \frac{\varphi'_0}{2} \tag{9}$$

where φ'_0 is the original in situ value of the angle of friction.

The coefficient of lateral earth pressure, K depends on the relative density, internal friction, and the pile installation method (Brødbæk et al. 2009; Fan and Long 2005). Different K values ranges from 0.5 to1 and 1 to 2 have been suggested for non-displacement and displacement driven piles, respectively (Hannigan et al. 2016; Wrana 2015). It can be suggested that these ranges for the cases of non-displacement and displacement piles are used in the proposed model to obtain acceptable range for p-y curves.

Reese method was proposed based on the results of only one static load test on an open-ended steel pipe pile with a specific length and diameter driven in one type of san soil. The developed p-y models in this paper demonstrate how different factors can affect the lateral behavior of the piles depending on the sand properties, pile properties, pile installation method, sand layering, and overburden pressure. Complexity of the problem suggests that instead of

obtaining one exact solution, one might calculate a range for p-y curves in depths. In this study, predictions of the proposed model based on K values between 0.4 and 1.0 showed acceptable performance for predicting the p-y curves for the open-ended pile tested at Mustang Island.

SUMMARY AND CONCLUSIONS

In this study, the lateral behavior of the piles driven in sand soils was investigated. For this purpose, a 3-D FE model was developed to evaluate the lateral capacity of piles driven in sand soils and develop p-y curves. The FE model was then used to conduct parametric study on the effects of different soil and pile properties on the p-y curves. Parametric study of the finite element results for piles showed that soil elastic modulus does not have effects on the value of ultimate soil resistance, p_u; but inversely changes the value of reference deflection, y_{ref}. y_{ref} is defined in this study as a displacement when the soil resistance almost reaches to p_u. The soil Poisson's ratio and soil-pile friction coefficient showed insignificant effects on the values of p_u and y_{ref}; while angle of friction, effective unit weight of the soil, coefficient of lateral earth pressure, and pile diameter showed direct relationship to p_u and y_{ref}.

The obtained p-y curves in different depths were used in nonlinear regression analysis and models composed of p_u and y_{ref} terms inside a composition of power and hyperbolic tangent functions for different pile shapes of circular, square, and rhombus were developed.

It was shown that the developed model is able to predict p-y curves for the cases of multidirectional lateral loading on square piles, soils with increasing modulus of elasticity with depth, soil layers with different modulus of elasticity and unit weight, and overburden pressure.

The developed model was evaluated using a full-scale pile test at Mustang Island. It was found that the measured data for p_u and initial slope for different depths is between model predictions using coefficient of lateral earth pressure, K of 0.4 and 1.0.

The most common method for predicting p-y curves in sands is Reese method. It was shown that analytical solution obtained by Reese is different from the measured data, thus Reese used the results of the Mustang Island test to propose a factor, A to fit the model to measured values. In this study, it was shown that this factor obtained for an open-ended pile with specific length and diameter driven in a specific sand type and it could be different for another condition. On the other hand, our proposed model is able to take into account different changes in soil properties such as friction angle (φ'), elastic modulus (E_s), and coefficient of lateral earth pressure (K).

Pile installation changes the properties of the surrounding soil such as φ' and K due to the soil disturbance, expansion, and shaking, friction and sliding between the pile and soil during pile driving, and gap creation between the pile and soil. It was suggested that for addressing these uncertainties in soil properties, the values of K in the proposed model for non-displacement and displacement driven piles be equal to 0.5 to 1.0 and 1.0 to 2.0, respectively. Using this approach, a range of p-y curves for different depths will be obtained which can be used for predicting the variety of pile behavior under lateral loading in sands.

ACKNOWLEDGMENTS

This research is funded by the Louisiana Transportation Research Center (LTRC Project No. 13-3GT) and Louisiana Department of Transportation and Development (State Project No. 1000103). The support of all LA DOTD engineers and LTRC researchers are gratefully acknowledged.

DATA AVAILABILITY STATEMENT

All data, models, and code generated or used during the study appear in the submitted article.

REFERENCES

Abaqus, F. 2017. Abaqus Inc. Providence, Rhode Island, United States.

API. 1989. Recommended practice for planning, designing, and constructing fixed offshore platforms. American Petroleum Institute.

API, R. 2014. 2A-WSD,(2014). Planning, Designing and Constructing Fixed Offshore Platforms-Working Stress Design.

Ashour, M., and Norris, G. 2000. Modeling lateral soil-pile response based on soil-pile interaction. Journal of Geotechnical and Geoenvironmental Engineering, **126**(5): 420-428.

Bethea, R.M. 2018. Statistical methods for engineers and scientists. Routledge.

Bogard, D., and Matlock, H. 1980. Simplified calculation of py curves for laterally loaded piles in sand. unpublished report), The Earth Technology Corporation, Inc., Houston, TX.

Brødbæk, K., Møller, M., Sørensen, S., and Augustesen, A.H. 2009. Review of py relationships in cohesionless soil.

Broms, B.B. 1966. Design of laterally loaded piles. Journal of Soil Mechanics & Foundations Div, **92**(Closure).

Budhu, M., and Davies, T.G. 1987. Nonlinear analysis of laterality loaded piles in cohesionless soils. Canadian Geotechnical Journal, **24**(2): 289-296.

Chatterjee, S., and Hadi, A.S. 2015. Regression analysis by example. John Wiley & Sons.

Christensen, D.S. 2006. Full scale static lateral load test of a 9 pile group in sand.

Conte, E., Troncone, A., and Vena, M. 2013. Nonlinear three-dimensional analysis of reinforced concrete piles subjected to horizontal loading. Computers and Geotechnics, **49**: 123-133.

Cox, W.R., Reese, L.C., and Grubbs, B.R. Field testing of laterally loaded piles in sand. *In* Offshore Technology Conference. 1974. Offshore Technology Conference.

Davisson, M., and Gill, H. 1963. Laterally loaded piles in a layered soil system. Journal of the Soil Mechanics and Foundations Division, **89**(3): 63-94.

DnV, D.N.V. 1980. Reles for the design, construction and inspection of offshore structures. Appendix F: Foundations. Hovik, Norway.

Duncan, J.M., Evans Jr, L.T., and Ooi, P.S. 1994. Lateral load analysis of single piles and drilled shafts. Journal of Geotechnical Engineering, **120**(6): 1018-1033.

Fan, C.-C., and Long, J.H. 2005. Assessment of existing methods for predicting soil response of laterally loaded piles in sand. Computers and Geotechnics, **32**(4): 274-289.

Georgiadis, M. Development of py curves for layered soils. *In* Geotechnical practice in offshore engineering. 1983. ASCE. pp. 536-545.

Georgiadis, M., Anagnostopoulos, C., and Saflekou, S. 1992. Centrifugal testing of laterally loaded piles in sand. Canadian Geotechnical Journal, **29**(2): 208-216.

Gibson, R. 1967. Some results concerning displacements and stresses in a non-homogeneous elastic half-space. Géotechnique, **17**(1): 58-67.

Haiderali, A.E., and Madabhushi, G. 2016. Evaluation of curve fitting techniques in deriving p–y curves for laterally loaded piles. Geotechnical and Geological Engineering, **34**(5): 1453-1473.

Hannigan, P., Rausche, F., Likins, G., Robinson, B., and Becker, M. 2016. Design and construction of driven pile foundations. Vol. I. Publication No. FHWA-NHI-16-009, US Department of Transportation, Federal Highway Administration.

Hansen, J.B. 1961. The ultimate resistance of rigid piles against transversal forces. Copenhagen, Denmark.

Ismael, N.F. 1990. Behavior of laterally loaded bored piles in cemented sands. Journal of Geotechnical

Engineering, **116**(11): 1678-1699.
Janbu, N. Soil compressibility as determined by odometer and triaxial tests. *In* Proc. Europ. Conf. SMFE. 1963. pp. 19-25.
Kondner, R.L. 1963. Hyperbolic stress-strain response: cohesive soils. Journal of the Soil Mechanics and Foundations Division, **89**(1): 115-144.
Matlock, H., and Reese, L.C. 1960. Generalized solutions for laterally loaded piles. Journal of the Soil Mechanics and Foundations Division, **86**(5): 63-94.
Mayerhof, G. 1976. Bearing capacity and settlemtn of pile foundations. Journal of Geotechnical and Geoenvironmental Engineering, **102**(ASCE# 11962).
Mayne, P.W., and Poulos, H.G. 1999. Approximate displacement influence factors for elastic shallow foundations. Journal of Geotechnical and Geoenvironmental Engineering, **125**(6): 453-460.
McClelland, B., and Focht, J.A. 1958. Soil modulus for laterally loaded piles. Transactions of the American Society of Civil Engineers, **123**(1): 1049-1063.
Motulsky, H.J., and Ransnas, L.A. 1987. Fitting curves to data using nonlinear regression: a practical and nonmathematical review. The FASEB journal, **1**(5): 365-374.
Murchison, J.M., and O'Neill, M.W. Evaluation of py relationships in cohesionless soils. *In* Analysis and design of pile foundations. 1984. ASCE. pp. 174-191.
NAVFAC, D. 1982. Foundations and earth structures. US Department of the Navy.
Ratkowsky, D.A., and Giles, D.E. 1990. Handbook of nonlinear regression models.
Reese, L., and Cox, W. 1969. Soil behavior from analysis of tests of uninstrumented piles under lateral loading. *In* Performance of deep foundations. ASTM International.
Reese, L.C., Cox, W.R., and Koop, F.D. 1974. Analysis of laterally loaded piles in sand. Offshore Technology in Civil Engineering Hall of Fame Papers from the Early Years: 95-105.
Reese, L.C., Cooley, L.A., and Radhakrishnan, N. 1984. Laterally Loaded Piles and Computer Program COM624G. TEXAS UNIV AT AUSTIN.
Rojas, R. 2013. Neural networks: a systematic introduction. Springer Science & Business Media.
Scott, R.F. 1980. Analysis of centrifuge pile tests; simulation of pile-driving.
Shojaeizadeh, A., Safaei, M.R., Alrashed, A.A., Ghodsian, M., Geza, M., and Abbassi, M.A. 2018. Bed roughness effects on characteristics of turbulent confined wall jets. Measurement, **122**: 325-338.
Smith, T.D. 1987. Pile horizontal soil modulus values. Journal of Geotechnical Engineering, **113**(9): 1040-1044.
Soleimani, S., Mousa, S., Codjoe, J., and Leitner, M. 2019. A Comprehensive Railroad-Highway Grade Crossing Consolidation Model: A Machine Learning Approach. Accident Analysis & Prevention, **128**: 65-77. doi:https://doi.org/10.1016/j.aap.2019.04.002.
Subramanian, N. 2008. Design of steel structures. Oxford University Press.
Tak Kim, B., Kim, N.-K., Jin Lee, W., and Su Kim, Y. 2004. Experimental load–transfer curves of laterally loaded piles in Nak-Dong River sand. Journal of Geotechnical and Geoenvironmental Engineering, **130**(4): 416-425.
Terzaghi, K. 1955. Evalution of conefficients of subgrade reaction. Géotechnique, **5**(4): 297-326.
Uncuoğlu, E., and Laman, M. 2011. Lateral resistance of a short rigid pile in a two-layer cohesionless soil. Acta Geotechnica Slovenica, **2**: 19-43.
Van Impe, W.F., and Reese, L.C. 2010. Single piles and pile groups under lateral loading. CRC press.
Wesselink, B., Murff, J., Randolph, M., Nunez, I., and Hyden, A. 1988. Analysis of centrifuge model test data from laterally loaded piles in calcareous sand. Engineering for calcareous sediments, **1**: 261-270.
Winkler, E. 1867. Die Lehre von Elastizitat und Festigkeit (The theory of elasticity and stiffness). H. Domenicus. Prague.
Wrana, B. 2015. Pile load capacity–calculation methods. Studia Geotechnica et Mechanica, **37**(4): 83-93.
WSD, A.R.A. 1993. Recommended Practice for Planning Designing and Constructing Fixed Offshore Platforms--WSD. API, Washington, DC, July.
Zhang, L., Silva, F., and Grismala, R. 2005. Ultimate lateral resistance to piles in cohesionless soils. Journal of Geotechnical and Geoenvironmental Engineering, **131**(1): 78-83.

Table 1. Summary of some p-y curve models for sand

Reference	Ultimate soil resistance (p_u)	Initial slope	Characteristic shape function
Reese et al. (1974)	$p_{u1} = \gamma' x \left[\frac{K_o\, x\, \tan\phi \sin\beta}{\tan(\beta-\phi)\cos\alpha} + \frac{\tan\beta}{\tan(\beta-\phi)}\,(D + x\tan\beta\tan\alpha) + K_o\, x\, \tan\beta\,(\tan\phi\sin\beta - \tan\alpha) - K_a\, D\right]$ $p_{u2} = K_a\, D\, \gamma' x(\tan^8\beta - 1) + K_o\, D\, \gamma' x \tan\phi \tan^4\beta$ $\alpha = \phi/2$ $\beta = 45 + \phi/2$ Reese Analytical model: $p_c = \min(p_{u1}, p_{u2})$ (using K_o=0.4 and $K_a = tan^2(45 - {}^{\varphi}/_{2})$) Reese model: $p_u = Ap_c$ & $p_m = Bp_c$ A and B: non-dimensional coefficients depending on x/D	$E_i = kx$	$p = E_i y\,,\ 0 < y < y_k$ $p = Cy^{1/n},\ y_k < y < y_m$ $p = p_m + \left(\frac{p_u - p_m}{y_u - y_m}\right)(y - y_m),\ y_m < y < y_u$ $y_k = \left(\frac{C}{E_i}\right)^{\frac{n}{1-n}}, y_m = \frac{D}{60}, y_u = \frac{3D}{80}$ $p = p_u,\ y > y_u$
Murchison and O'Neill (1984)	$p_c = p_c$(Reese Analytical model)	$E_{py} = kx$	$p = \eta A p_c \tanh(\frac{E_{py}}{\eta A p_u} y)$
Ismael (1990)	$p_u = C_p \sigma_p D$ $\sigma_p = 2S_u \tan([45 + \phi]/2) + \sigma'_v \tan^2([45 + \phi]/2)$	-	$p = 0.5 p_u \left(\frac{y}{y_{50}}\right)^{\frac{1}{3}} \le p_u$ $y_{50} = 2.5\varepsilon_{50} D$
Georgiadis et al. (1992)	$p_u = p_u$(Reese model)	$k = n_h x$	$p = \frac{y}{\frac{1}{k} + \frac{y}{p_u}}$
Tak Kim et al. (2004)	$p_u = K_p D \gamma' x^n$	$k = n_h x$	$p = \frac{y}{\frac{1}{k} + \frac{y}{p_u}}$
API (2014)	$p_{u1} = (C_1 x + C_2 D)\gamma' x\,,\ p_{u2} = C_3 D \gamma' x$ $p_c = \min(p_{u1}, p_{u2})$	$E_{py} = kx$	$p = \eta A p_c \tanh(\frac{E_{py}}{\eta A p_u} y)$
*S_u is undrained shear strength, γ' is effective unit weight, x is depth, D is pile width, ε_{50} is strain corresponding to S_u, k is modulus of horizontal subgrade reaction, n_h is coefficient of horizontal subgrade reaction, K_o is coefficient of earth pressure at rest, K_a is coefficient of active earth pressure, K_p is coefficient of passive earth pressure, ϕ is friction angle of soil			

Table 2. Model parameters used in the finite element analysis

modulus of elasticity of soil (E_s) MPa	Poisson's ratio of soil (ν)	angle of friction of soil (φ')	effective unit weight of soil (γ') kN/m^3	soil-pile interface coefficient (μ)	coefficient of lateral earth pressure (K)	pile diameter (D) m
9.6	0.2	25	7.9	0.2	0.5	0.30
23.9*	**0.3**	**30**	**9.4**	**0.3**	0.75	0.61
47.9	0.4	35	15.7	0.4	**1.0**	**0.91**
95.8		40	18.9		2.0	1.22

* **Bold values represent the reference case.**

Table 3. Developed model for p-y curves in sands for different pile shapes

Pile shape	p-y curve function	ultimate resistance, p_u, and reference displacement, y_{ref}
circular	$p = p_u \tanh\left(\left(\frac{2y}{y_{ref}}\right)^{0.8}\right)$	$p_u = 21299 \times (x/L_0)^{0.9} \times \tan^{1.2}\varphi' \times (\gamma'/\gamma_w)^{0.5} \times K^{0.8} \times (D/L_0)$ $y_{ref} = 44.9 \times (x/L_0)^{0.8} \times (P_0/E_s) \times \tan^{1.4}\varphi' \times (\gamma'/\gamma_w)^{0.6} \times K^{0.9} \times (D/L_0)^{0.9}$
square	$p = p_u \tanh\left(\left(\frac{2y}{y_{ref}}\right)^{0.66}\right)$	$p_u = 24044 \times (x/L_0)^{0.8} \times \tan^{1.2}\varphi' \times (\gamma'/\gamma_w)^{0.5} \times K^{0.8} \times (D/L_0)$ $y_{ref} = 117.6 \times (x/L_0)^{0.5} \times (P_0/E_s) \times \tan^{1.4}\varphi' \times (\gamma'/\gamma_w)^{0.6} \times K^{0.9} \times (D/L_0)^{0.9}$
rhombus	$p = p_u \tanh\left(\left(\frac{2y}{y_{ref}}\right)^{0.8}\right)$	$p_u = 20814 \times (x/L_0)^{0.8} \times \tan^{1.2}\varphi' \times (\gamma'/\gamma_w)^{0.5} \times K^{0.8} \times (D/L_0)$ $y_{ref} = 60.6 \times (x/L_0)^{0.5} \times (P_0/E_s) \times \tan^{1.4}\varphi' \times (\gamma'/\gamma_w)^{0.6} \times K^{0.9} \times (D/L_0)^{0.9}$

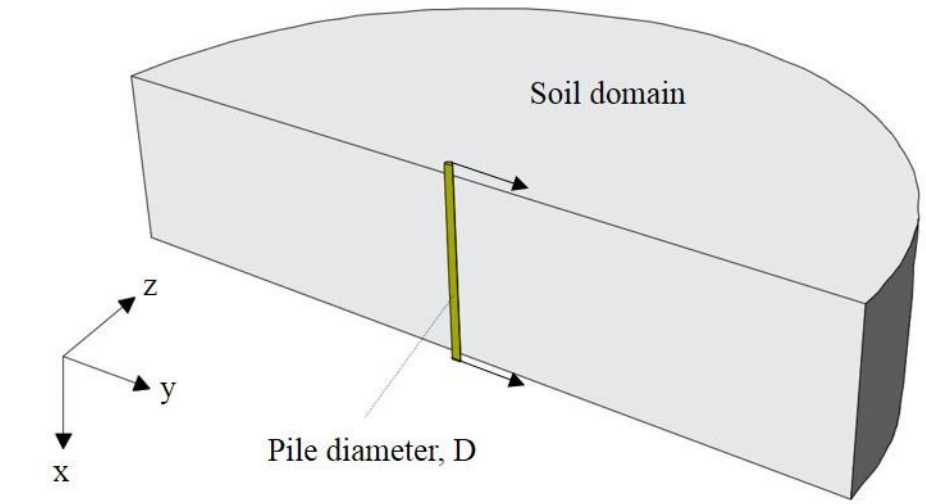

(a)

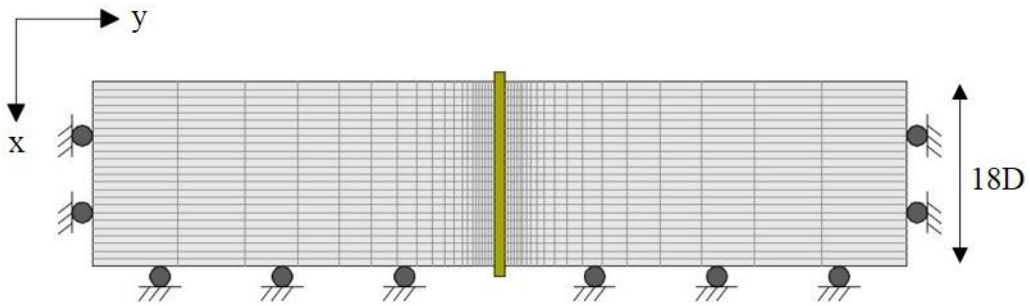

(b)

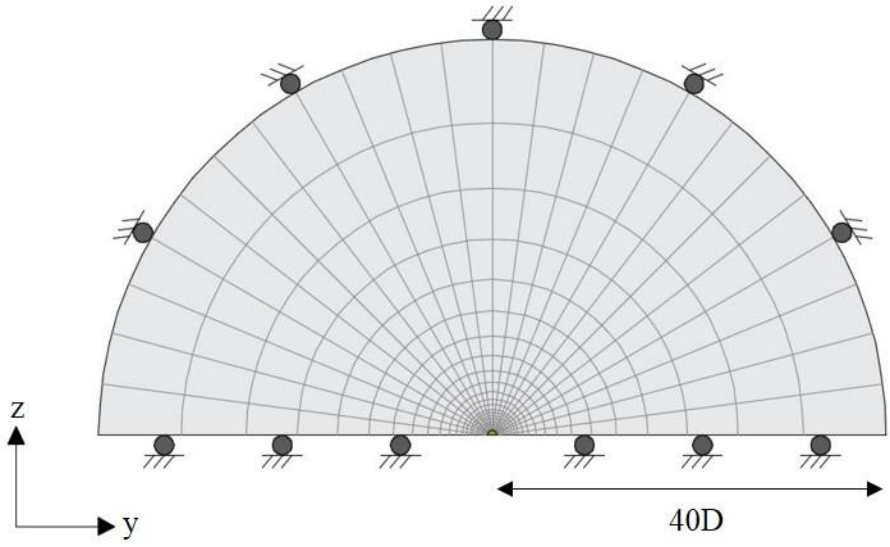

(c)

Figure 1. (a) Three-dimensional schematic of the pile-soil model for finite element analysis (b) section xy of the model (c) section yz of the model

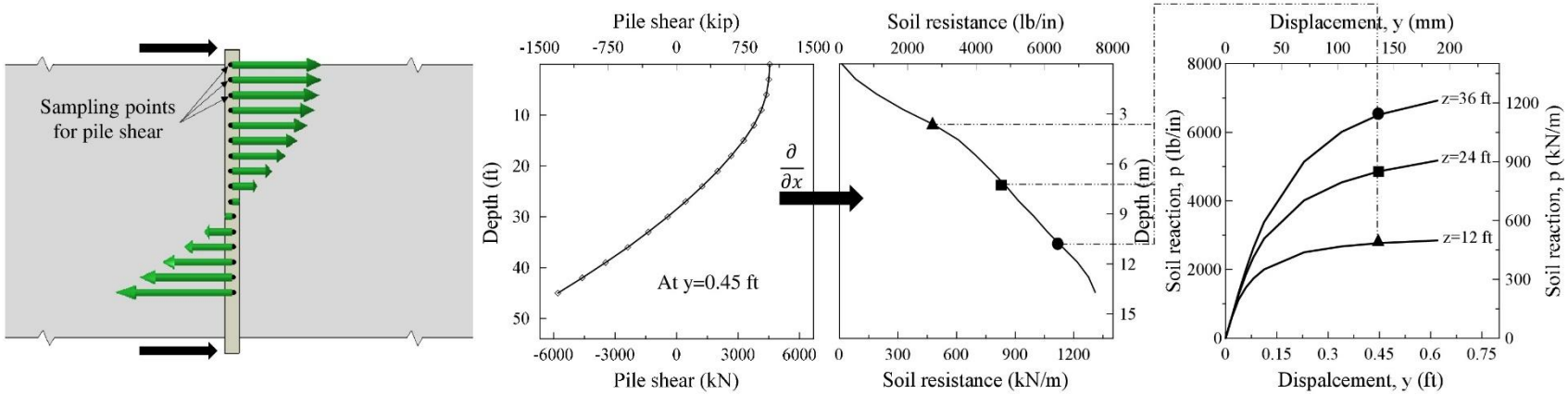

Figure 2. Procedure of obtaining soil resistance from results of finite element at a specific displacement for calculating p-y curves

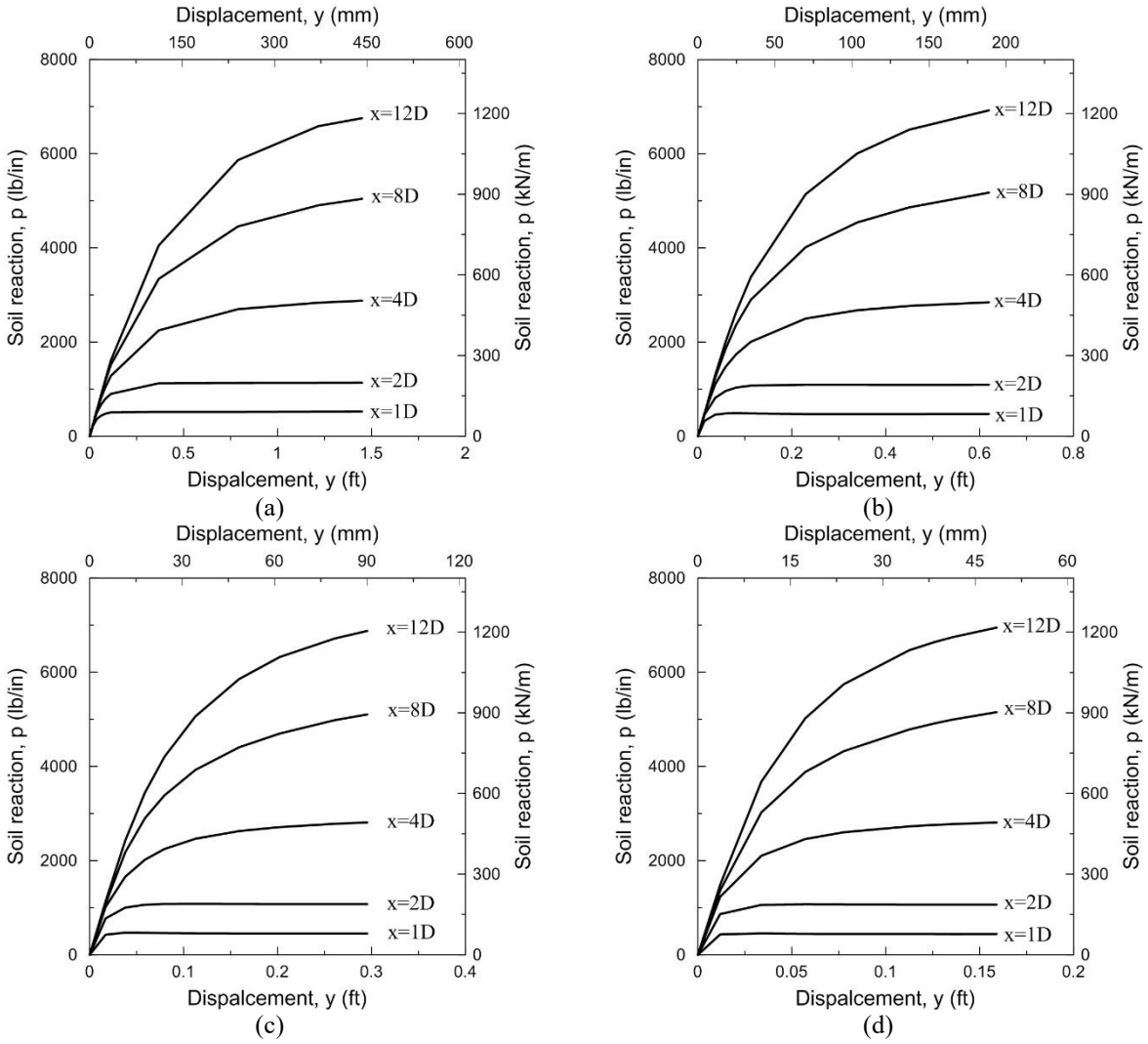

Figure 3. The p-y Curves for piles in sands with elastic modulus (E_s) (a) 9.6 (b) 23.9 (c) 47.9 (d) 95.8 MPa

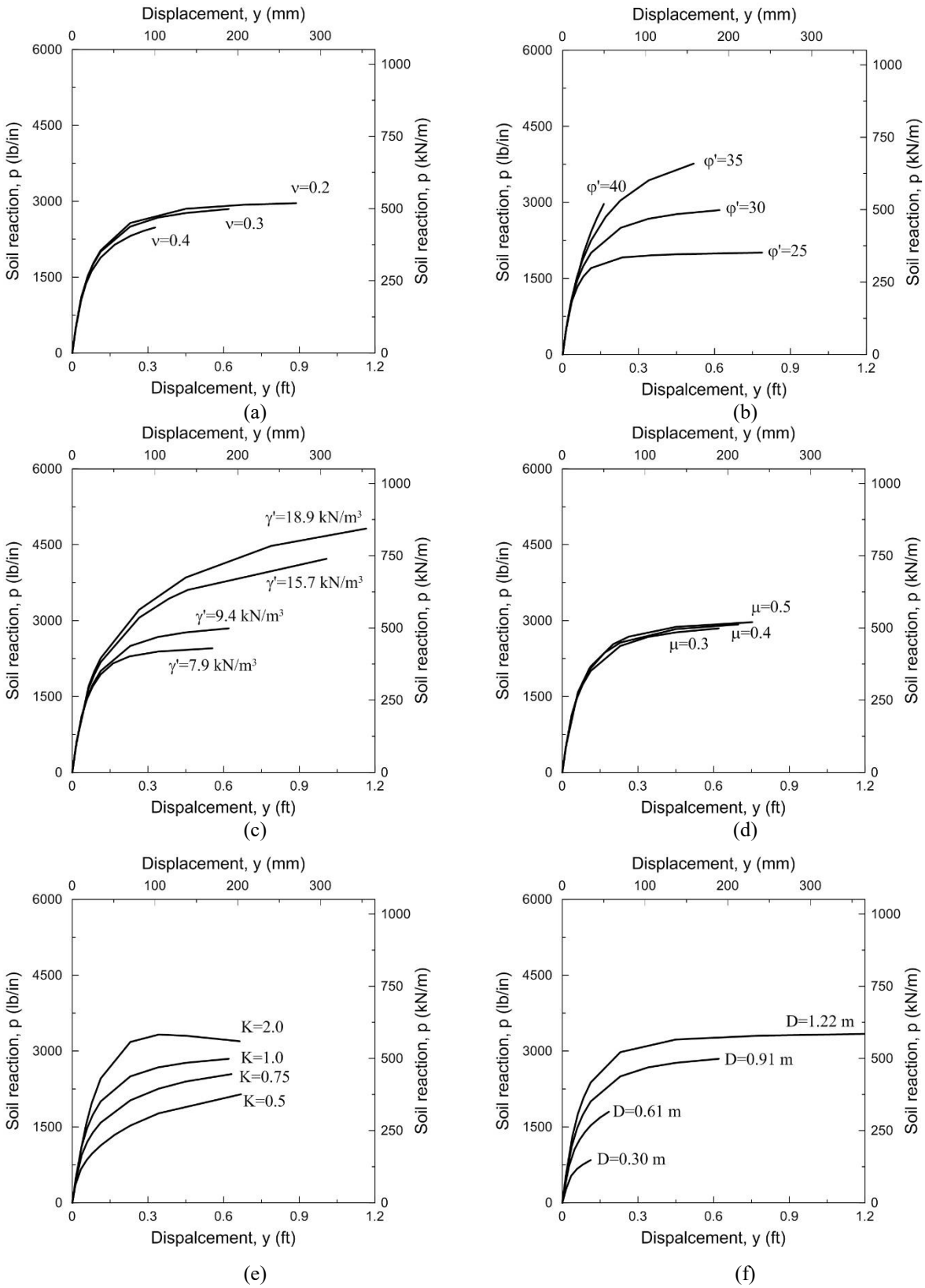

Figure 4. Effects of (a) Poisson's ratio (b) friction angle (c) effective unit weight (d) interface friction (e) coefficient of lateral earth pressure (f) pile's diameter on the p-y curve at depth, x=3.66 m

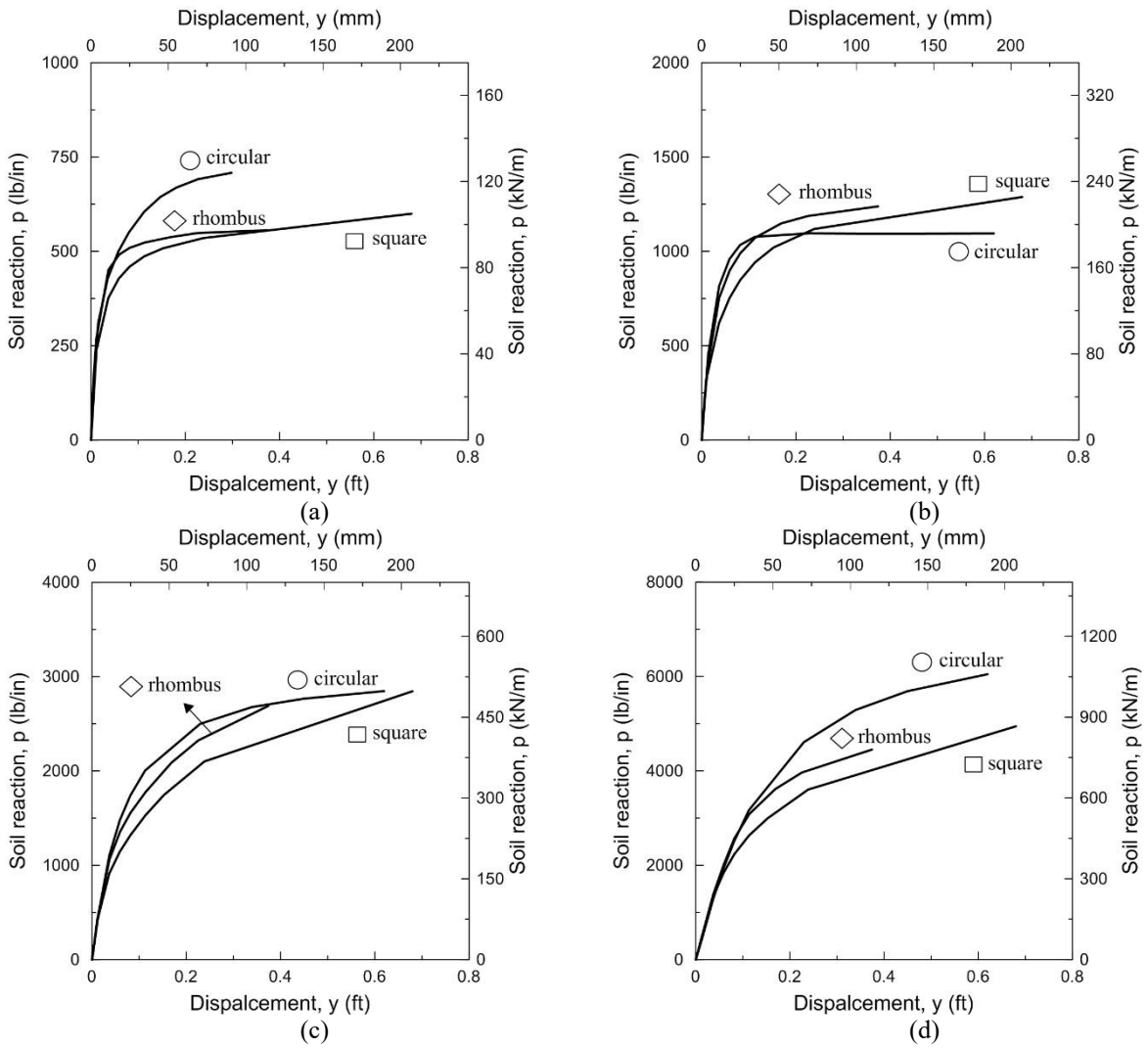

Figure 5. The p-y curves for circular, square, and rhombus pile at depth (a) 0.91 (b) 1.83 (c) 3.66 (d) 9.14 m

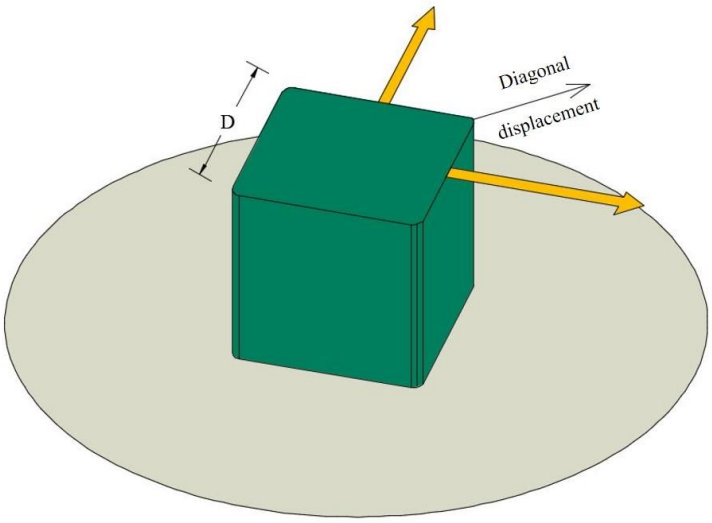

Figure 6. Square piles under multidirectional lateral loading

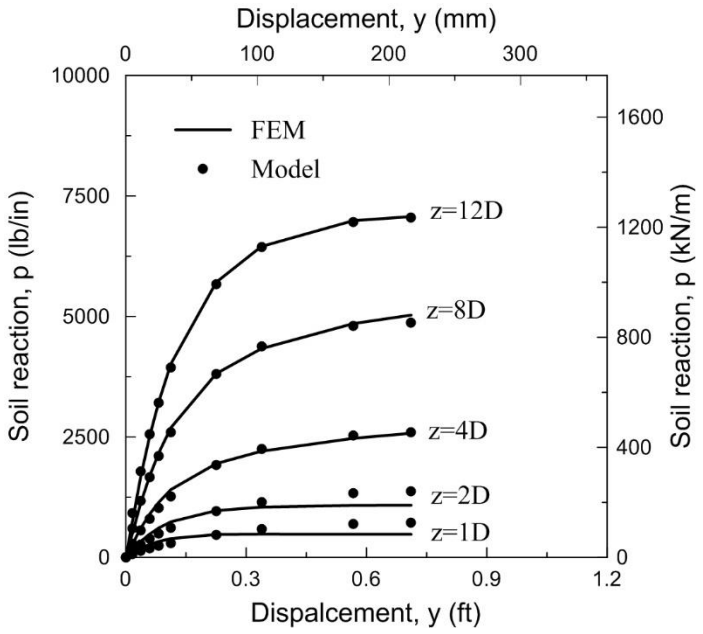

Figure 7. Comparison between p-y curves of Finite Element and model for the case of E_s increases linearly to 23.9 MPa (1,000,000 psf) at Depth 16.5 m (54 ft)

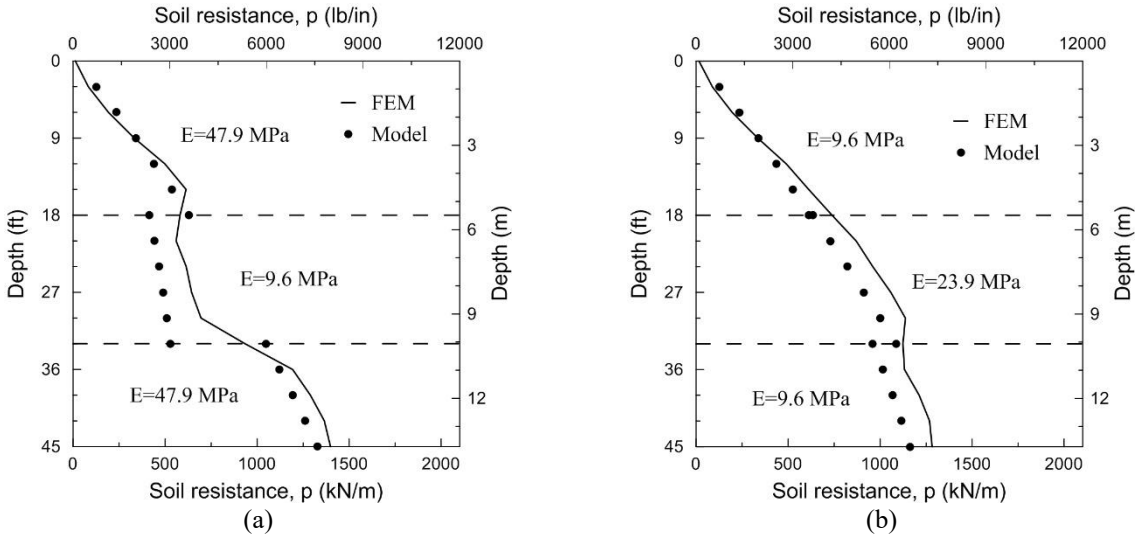

Figure 8. The value of soil resistance, p for piles in layered sands with different modulus of elasticity

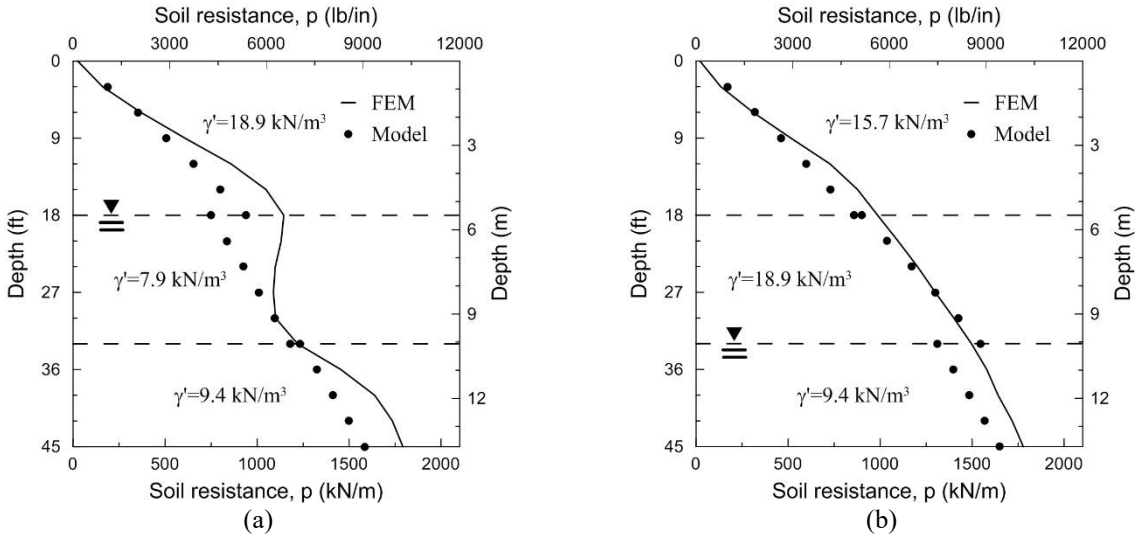

Figure 9. The value of soil resistance, p for piles in layered sands with different unit weight

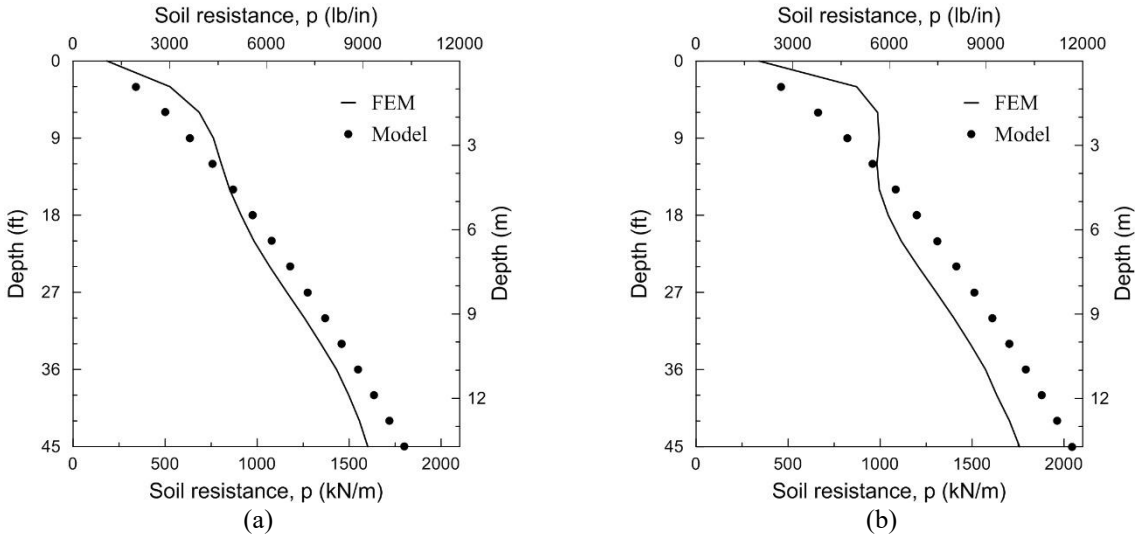

Figure 10. The value of soil resistance, p for piles in sands with overburden pressure, σ'_0 equal to (a) 47.88 (b) 95.76 kPa

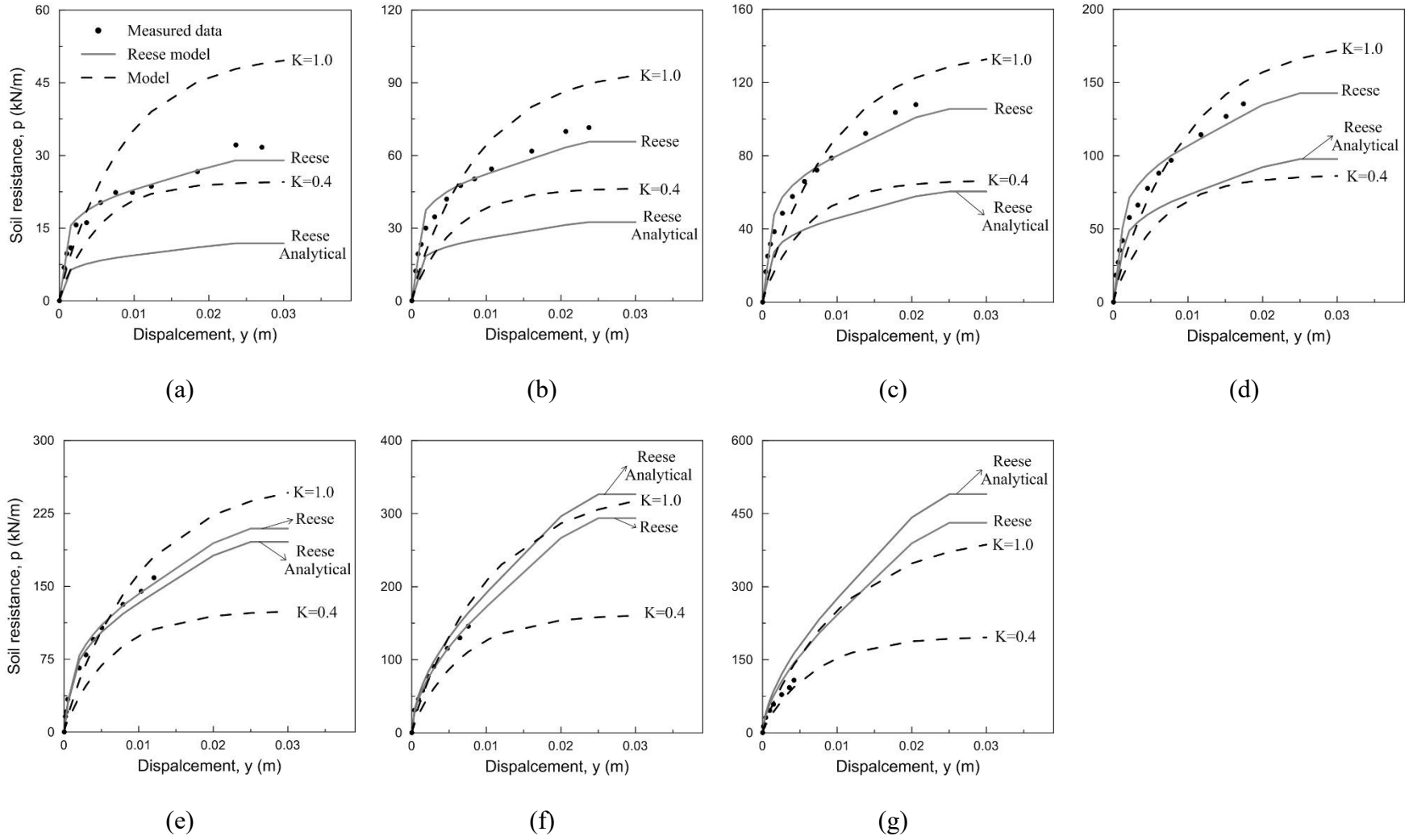

Figure 11. Comparison between the measured and predicted p-y curves for depths, x= (a) 0.30 m (b) 0.61 m (c) 0.91 m (d) 1.22 m (e) 1.83 m (f) 2.44 m (g) 3.05